COUPLED HELICON-CYCLOTRON MODES: THEORY AND EXPERIMENT

Francis F. Chen, Donald Arnush, John D. Evans, and David D. Blackwell

University of California, Los Angeles, California 90095-1594, USA

Helicon discharges, noted for their exceptional ionization efficiency and high densities, are now used in plasma processing. The weak magnetic fields used in plasma etch reactors lead to non-negligible values of $\delta = \omega/\omega_c$, necessitating the addition of electron mass m effects to simple helicon theory. This introduces a second root with the same parallel wavenumber k, which we shall call a Trivelpiece-Gould (TG) mode, and which is coupled to the usual helicon (H) wave by the boundary condition. The TG mode is an electron cyclotron wave in a bounded cylinder and is the same as the classical Trivelpiece-Gould mode but with electromagnetic corrections. For $\delta << 1$, the TG wave propagates at large angles to the magnetic field $B_0\,\hat{\mathbf{z}}$, so it propagates inwards from the wall with short radial wavelength and is rapidly absorbed. Thus, the H wave, itself weakly damped, heats the plasma electrons by transferring its energy to the strongly damped TG mode. We believe that this mechanism, first pointed out by Shamrai and Taranov [1], accounts for the efficacy of helicon sources rather than Landau damping, as was originally thought [2].

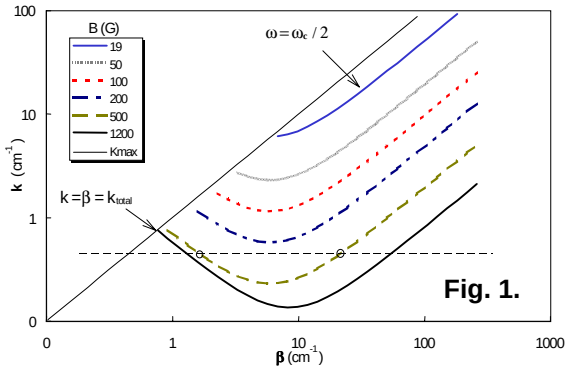

Fig. 1.

The effects of finite δ were first treated by Davies [3] and Boswell [4] and have recently been re-examined by Chen and Arnush [5]. The normal mode situation is summarized by Fig. 1. Here k is $k_\parallel$ and β is the total wavenumber $(k_\perp^2 + k_\parallel^2)^{1/2} \approx k_\perp$. For each k and B_0, there are two possible values of β (dashed line), the smaller one corresponding to the normal H mode, and the larger one to the TG mode. As B_0 is decreased, the roots approach each other, and the wave pattern of the H mode is significantly altered by the TG mode. Finally, for fields such that $\omega_c < 2\omega$, only the TG mode propagates and is coupled to an evanescent H wave.

Examples of radial B_z profiles for given k and azimuthal mode number m for uniform density are shown in Figs. 2a and 2b for the H and TG waves alone and for their sum. At the higher field of Fig. 2a, the radial wave numbers are disparate, and TG mode can be seen as a rapid oscillation. In practice, this would be damped out near the surface at $r = a$ and would not be detectable experimentally. At the lower field of Fig. 2b, however, the two waves have comparable wavelengths, and the profile of the total wave (the top curve) would be easily distinguishable from that of the H wave alone (the bottom curve). This is the case we tried to probe experimentally.

The equation followed by the wave magnetic field **B** is

$$\delta\nabla\times\nabla\times\mathbf{B} - k\nabla\times\mathbf{B} + k_w^2\mathbf{B} = u(r)[-\delta_0\hat{\mathbf{r}}\times\nabla\times\mathbf{B} + i(\nabla\times\mathbf{B})_r\hat{\mathbf{z}}\ , \qquad (1)$$

where δ and δ_0 are essentially ω/ω_c but with imaginary parts due to damping, $u(r)$ is the radial density gradient $-n_0'/n_0$, and $k_w \equiv (\omega_p/c)(\omega/\omega_c)^{1/2}$ is the whistler wave k in free space. We have developed a simple program [6] for solving Eq. (1) in an infinite, uniformly magnetized

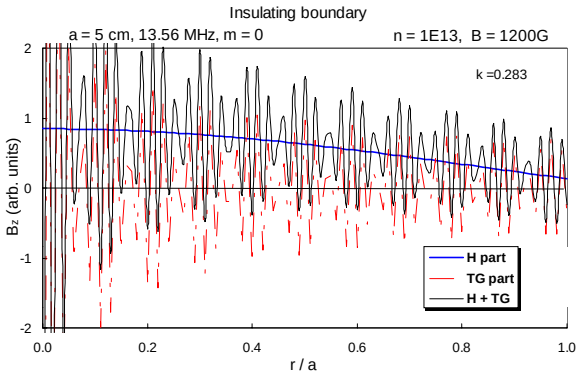

Fig. 2a

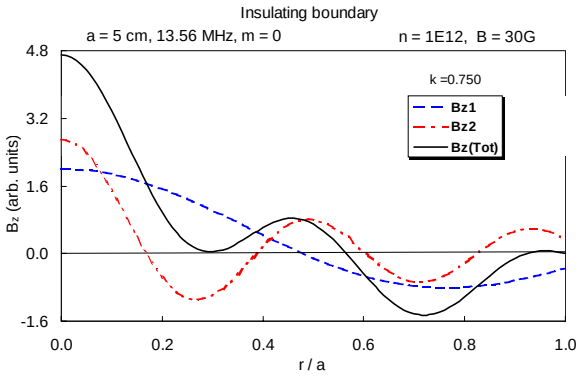

Fig. 2b

cylinder with arbitrary radii a for the plasma, $b > a$ for the antenna, and $c > b$ for the conducting boundary. Arbitrary $u(r)$ and antenna surface currents **K** are treated, as are electron collisions with ions and neutrals; however, ion motions, end boundaries, and axial density variations are neglected. Displacement currents are treated exactly, but they are omitted for convenience in calculations where they are obviously negligible. The Fourier components (m, k) can be expressed in the form

$$\mathbf{B}(r) = \frac{H_2\mathbf{b}_1(r) - H_1\mathbf{b}_2(r)}{D(a,c,k)} K_\theta \,, \tag{2}$$

where K_θ is the transform of **K**, and the subscripts 1 and 2 correspond to the H and TG modes in cases where they are not totally mixed. Eq. (1) needs to be solved only to obtain the basis functions $\mathbf{b}_1$ and $\mathbf{b}_2$. The relative amplitudes H_j and the denominator D depend only on the surface values of $\mathbf{b}_j$ and the geometrical constants. Thus, once the $\mathbf{b}_j$ are found for given $u(r)$, it is trivial to try different antennas. Figs. 3-6 give TG-relevant results from this formulation. Figs. 3 and 4 show the B_z and J_z profiles for the H and TG modes and their phased sum.

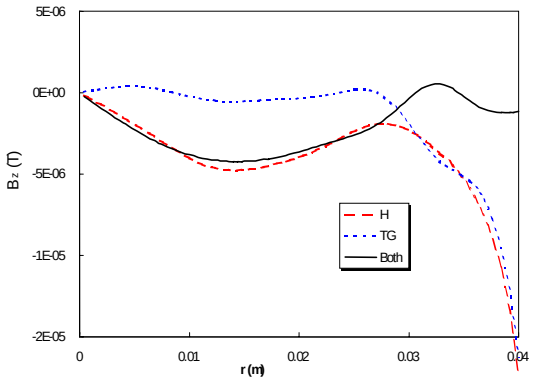

Fig. 3.

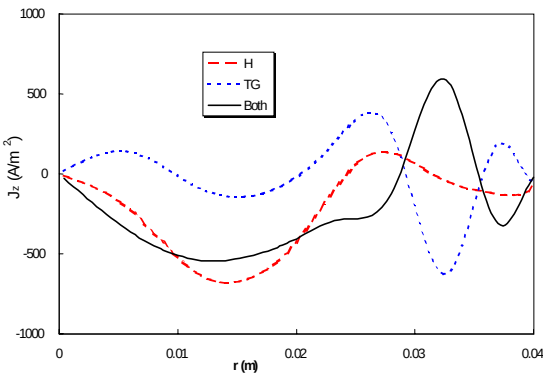

Fig. 4.

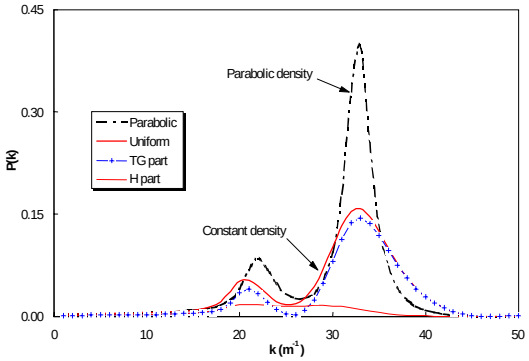

Fig. 5.

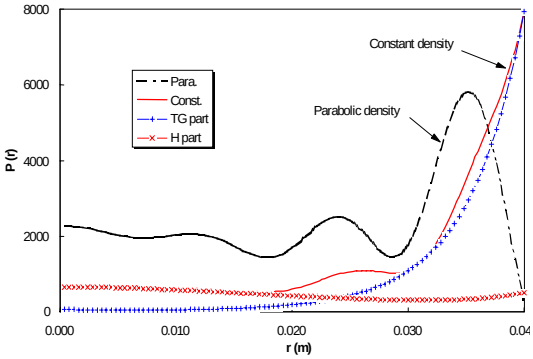

Fig. 6.

[100G, 10^{12} cm^{-3} parabolic, 3mTorr Ar, T_e = 3eV, a = 4cm, 13.56MHz, m = 1]

Though the H mode has relatively small B_z except near the edge, its currents are significant because $J_z \approx \beta B_z$, and it has large β. Since the power deposition $P(r) \propto J_z^2$, the TG mode plays an important part in $P(r)$ even when it cannot be seen. This is borne out Figs. 5 and 6, which show $P(k)$ and $P(r)$ for uniform and parabolic density profiles, as well as the H and TG contributions in the uniform case.

An attempt to detect the TG mode in a previously described [7] 10-cm diam helicon source engendered two problems: 1) elimination of capacitive coupling, which is not included in the theory but had been found [7] to be important; and 2) difficulty in finding a regime of quiescent and reproducible operation at very low B-fields. A Faraday shield was made to fit an $m = 1$ helical antenna (Fig. 7), but results were sensitive to the way the shield was grounded at RF frequencies, as evidenced by the lack of symmetry in the field magnitude. To achieve credible results, the antenna was reduced to a single-loop $m = 0$ antenna with azimuthal symmetry, and a reproducible operating condition was found at 30G. Measurements were made with offset Langmuir and magnetic probes along the axis. Fig. 8 shows the radial variation of B_z (points), compared with the calculated curve for a uni form plasma (solid curve) and the curves for the H and TG parts. At this density, the TG mode is heavily damped, and was not possible to resolve the difference at the edge. Fig. 9 shows the axial variation of B_z (points), compared with the computed curve (solid) and the curve for the H mode alone (dashed). However, the theory does not take into account the variation of density along z. The experiment needs to be repeated at lower density, where the TG mode is less damped.

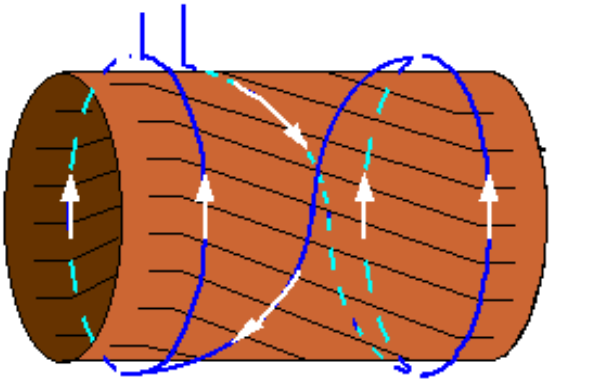

Fig. 7.

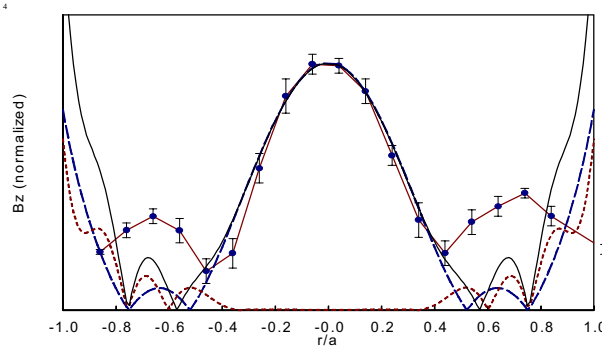

Fig. 8.

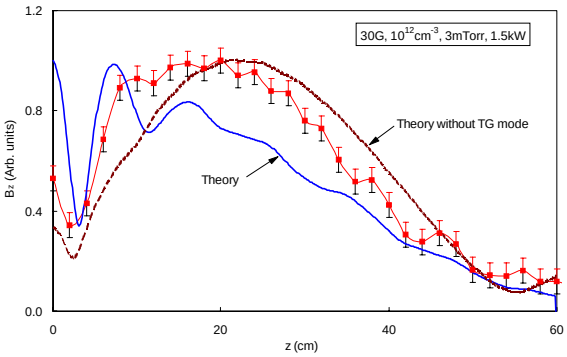

Fig. 9.

At low B-fields, we have previously found a low-$\mathbf{B}_0$ (LB) density peak in several helicon sources [8], and we believe this is indicative of the presence of the TG mode at low $\mathbf{B}_0$. We have now seen the LB peak in a multi-tube helicon source in a nonuniform magnetic field. The apparatus, shown in Fig. 10 and described elsewhere [9], consists of 6 sources surrounding a central source. Scans with the rotatable ion collector array have revealed no $m = 6$ azimuthal asymmetries, thus showing that a uniform plasma can be produced with an array of many helicon sources. Fig. 11 shows n-B curves measured in this device, and the low-field peak can be seen at intermediate RF powers. Thus, it appears that strong coupling to the TG mode enhances power absorption in a variety of devices. An LB peak can be seen in the com-

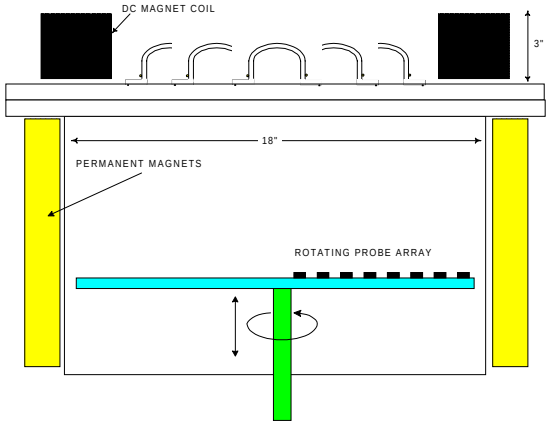

Fig. 10.

putations of the plasma loading resistance $R_p(n,B)$ for a short plasma by Shamrai *et al*. [10], but this is not the same as a low-field *density* peak. Cho and Kwak [11] have pointed out that the circuit losses i^2R_c must be taken into account. Since the plasma losses P_{out} increase with n while the power P_{in} into the plasma is equal to i^2R_{eff}, where $R_{eff} \equiv R_p/(R_p + R_c)$, there can be a peak in n only if there is a peak in R_{eff}. We have computed R_{eff} (B) for various densities in a long plasma, assuming $R_c = 0.2\Omega$ (Fig. 12). This shows an LB peak which vanishes at higher power (higher n), as is seen at higher P_{rf} than is shown in Fig. 11.

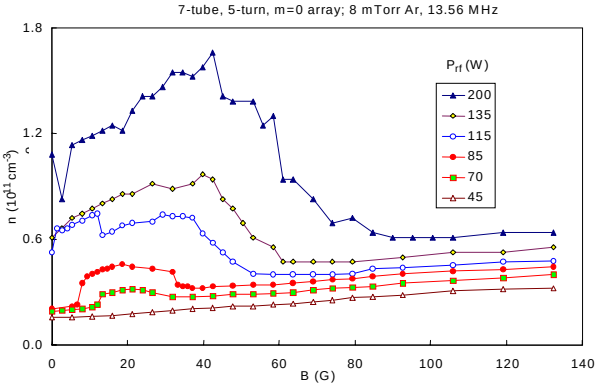

Fig. 11.

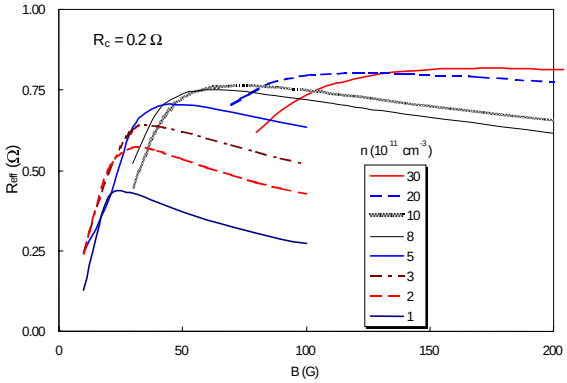

Fig. 12.

In conclusion, we have shown theoretically that the TG mode accounts for the major part of RF power absorption in helicon discharges, even when this wave has large amplitude only near the surface. The TG wave can, in principle, be detected at very low magnetic fields, but attempts at this have given inconclusive results so far. Existence of a low-B density peak has been confirmed both experimentally and theoretically. This work was supported by the National Science Foundation and the Semiconductor Research Corporation, and we thank Dr. George R. Tynan for his help.

---

[1] K.P. Shamrai and V.B. Taranov, Plasma Sources Sci. Technol. **5**, 474 (1996).
[2] F.F. Chen, Plasma Phys. Control. Fusion **33**, 339 (1991).
[3] B.J. Davies, J. Plasma Phys. **4**, 43 (1970).
[4] R.W. Boswell, Aust. J. Phys. **25**, 403 (1972).
[5] F.F. Chen and D. Arnush, Phys. Plasmas **4**, 3411 (1997).
[6] D. Arnush and F.F. Chen, Phys. Plasmas **5**, 1239 (1998).
[7] D.D. Blackwell and F.F. Chen, Plasma Sources Sci. Technol. **6**, 569 (1997).
[8] F.F. Chen, X. Jiang, J.D. Evans, G. Tynan, and D. Arnush, Plasma Phys. Control. Fusion **39**, A411 ('97).
[9] F.F. Chen and J.D. Evans, "Performance of a multi-tube, large-area helicon source", *in Proc. Plasma Etch Users Group* (NCCAVS, 150 W. Iowa Ave., Suite 104, Sunnyvale, CA 94086.
[10] K.P. Shamrai *et al*., J. Vac. Sci. Technol A **15**, 2864 (1997).
[11] S. Cho and J.G. Kwak, Phys. Plasmas **4**, 4172 (1997).